Contents lists available at ScienceDirect

# Biochemistry and Biophysics Reports

# Integrin molecular tension required for focal adhesion maturation and YAP nuclear translocation

Cheng-Yu Chang Chien [a], Shih-Hua Chou [a], Hsiao-Hui Lee [a,b,*]

[a] Department of Life Sciences and Institute of Genome Sciences, National Yang Ming Chiao Tung University, Taiwan
[b] Center for Intelligent Drug Systems and Smart Bio-devices (IDS2B), National Yang Ming Chiao Tung University, Taiwan

## ARTICLE INFO

## ABSTRACT

Focal adhesions (FAs) provide the cells linkages to extracellular matrix (ECM) at sites of integrins binding and transmit mechanical forces between the ECM and the actin cytoskeleton. Cells sense and respond to physical stimuli from their surrounding environment through the activation of mechanosensitive signaling pathways, a process called mechanotransduction. In this study, we used RGD-peptide conjugated DNA tension gauge tethers (TGTs) with different tension tolerance ($T_{tol}$) to determine the molecular forces required for FA maturation in different sizes and YAP nuclear translocation. We found that the limitation of FA sizes in cells seeded on TGTs with different $T_{tol}$ were less than 1 μm, 2 μm, 3 μm, and 6 μm for $T_{tol}$ values of 43 pN, 50 pN, 54 pN, and 56 pN, respectively. This suggests that the molecular tension across integrins increases gradually as FA size increases throughout FA maturation. For YAP nuclear translocation, significant YAP nuclear localization was observed only in the cells seeded on the TGTs with $T_{tol} \geq 54$ pN, but not on TGTs with $T_{tol} \leq 50$ pN, suggesting a threshold of molecular force across integrins for YAP nuclear translocation lies in the range of 50 pN–54 pN.

## Author contribution

H.-H. L. designed, administered, & conducted the experiments, and wrote the paper; C.-Y. C. C., carried out the fabrication of RGD-TGTs and experiments of FA analysis, S.-H. C conducted the experiments of YAP nuclear translocation.

## 1. Introduction

The interactions of adherent cells with the extracellular matrix (ECM) mediated by the integrins are essential for many cellular functions. Cellular tension is modulated by extracellular mechanical stimuli through changes of cytoskeletal organization and molecular processes which in turn alter cell behavior as well as gene expression [1–4]. The response of cells to physical stimuli of the ECM is a general phenomenon affecting tissue development and homeostasis [5,6]. Focal adhesions (FAs) provide the cells linkages to ECM at sites of integrins binding and transmit mechanical forces between the ECM and the actin cytoskeleton [7,8]. The engagement of integrins with ECM proteins activates the integrins to recruit multiple proteins to form nascent adhesions.

Thereafter, some adhesions disassemble, while other adhesions mature in a force-dependent manner [9]. A reduction in contractility leads to FA disassembly, whereas an enhancement in contractility causes FA stabilization and maturation. The mechanical forces also modulate mechanosensitive pathways by changing protein conformation to enhance their biochemical activities or protein-protein interactions to fine-tune mechanotransduction [10–14]. Thus, the ligand-engaged integrins, adaptor proteins at FAs, actin filaments, myosin motors pulling on actin filaments, and the mechanosensitive molecules work coordinately as a molecular clutch system [15], which determines not only force transmission but also force transduction, as well as the activation of downstream signals such as FA dynamics and gene expression for the corresponding cell behavior [16].

It is well known that the nuclear translocation of Yes-associated protein (YAP) can be driven by mechanical forces [17,18]. YAP is a transcriptional regulator that plays critical roles in cancer, development, regeneration, and organ size control [19–22]. The function of YAP is mainly controlled by its localization in either the cytoplasm or the nucleus, and regulated by both biochemical and mechanical cues [23]. YAP is biochemically regulated by Hippo signaling pathway through protein

phosphorylation [24]. YAP is also regulated by many mechanical cues that requires cytoskeletal integrity, which involves different adhesive and cytoskeletal structures, including myosin contractility and the linker of nucleoskeleton and cytoskeleton (LINC) complex [25–28]. It has been reported that force applied to the nucleus directly triggers YAP nuclear entry by decreasing the mechanical restriction of nuclear pores to molecular transport [29]. Therefore, the YAP nuclear translocation is driven by the adhesion-mediated cellular forces. A systematic investigation of the interplays between the FA-mediated forces and various mechanosensitive cellular events, such as YAP activation, will provide a deeper understanding of the mechanotransduction in cancer and in other related diseases.

Different technologies have been developed to study the mechanics of the cell-matrix interaction. Traction force microscopy (TFM) technique measures cells deformation on elastic polymers or microstructures to provide the information about force magnitude and organization in living cells [30,31]. Single molecule force spectroscopy (SMFS) techniques, such as atomic force microscopy (AFM) and optical or magnetic tweezers, applies external forces to probe the mechanics of single molecule in vitro [32,33]. The fluorescence resonance energy transfer (FRET)-based tension sensors measure the mechanical tension across the designed molecules, such as vinculin tension sensor, in living cells [34–36]. In addition to these technologies, Wang and Ha have developed the tension gauge tether (TGT) approach in which the ligand is immobilized to a surface through a rupturable tether to define the molecular forces required to activate integrin for cell adhesion and the molecular tension threshold to activate Notch signaling [37]. Using a range of integrin ligand-conjugated TGTs with tunable tension tolerances ($T_{tol}$), they observed that integrin experienced about 40 pN during initial adhesion [37]. They also provided evidence that links molecular forces at the cell-substrate interface to the extent of cell spreading [38].

In this study, we used the TGT approach to measure the force required for FA maturation in different size and YAP nuclear translocation, two elementary cellular processes that depend on integrin-mediated adhesion and controlled by myosin II-mediated forces. Our results reveal that (1) the molecular tension on integrin increases with the FA size during FA maturation, and (2) the YAP nuclear translocation requires a threshold of molecular tension in the range of 50–54 pN.

## 2. Materials and methods

### 2.1. Cell culture

Mouse embryonic fibroblasts (MEFs) were maintained in Dulbecco's modified Eagle's medium (DMEM) supplemented with 10% (v/v) of fetal bovine serum (FBS) and antibiotics (10 unit/ml of Penicillin and 0.1 mg/ml of Streptomycin) in a humidified atmosphere of 5% CO2/ 95% air at 37 °C. Cells were allowed to attach onto the RGD-conjugated TGTs or glass coverslips coated with 10 μg/ml of fibronectin (FN) or 0.1 mg/ml of poly-L-lysine (PLL) in the completed culture media.

### 2.2. Reagents and antibodies

Cyclic peptide RGDfk-NH2 was obtained from Peptides International (Louisvile, KY, USA), biotin-labeled bovine serum albumin (BSA), Hoechst-33342, and glutaraldehyde were from Sigma-Aldrich (Louis, MO, USA), mouse anti-paxillin antibody and fibronectin were from BD Biosciences (San Jose, CA, USA), Neutravidin and Sulfo-SMCC were from Thermo Fisher Scientific (Waltham, MA, USA), Phalloidin was from molecular probe, (Grand Island, NY, USA), mouse anti-YAP monoclonal IgG was from Santa Cruz Biotechnology (Dallas, Texas, TX, USA), CF568 goat anti-mouse IgG was from Biotium, Inc. (Fremont, CA, USA).

### 2.3. Fabrication of RGD-conjugated TGTs

To create the TGTs linked ligand for integrins, we conjugated cyclic-RGDfK peptide to a DNA strand of a dsDNA as a rupturable tethers, as was described elsewhere [37]. The single-stranded DNA oligomers were purchased from MDBio, Inc. (Taipei, Taiwan). The sequence of forward ssDNA is: 5-/Cy5/CAC AGC ACG GAG GCA CGA CAC/3ThioMC3-D/-3; where 5′ was conjugated with Cy5 and 3' was modified with a reactive thiol group. The cyclic-RGDfK peptide and forward ssDNA were conjugated to each other through hetero-bifunctional crosslinker Sulfo-SMCC. The RGD-conjugated ssDNA was then purified and then annealed with different complementary reversed ssDNA which have biotin labeling at different positions to form the dsDNA TGT constructs. The annealing efficiency and the quality of each dsDNA TGT constructs were checked by 15% polyacrylamide gel electrophoresis (Fig. S1).

Glass coverslips were functionalized with an array of TGTs [38]. Briefly, the silane-coated slides were incubated with 0.1 mg/ml of biotin-BSA at 4 °C for overnight. Slides were washed with PBS and then incubated with 0.5% of glutaraldehyde for 10 min at room temperature. After several washes, the surface was blocked by 3% of BSA for 30 min, followed by incubation with neutravidin for 30 min at room temperature. After washing again with PBS, 1 μM of RGD-conjugated dsDNA were spotted on the on the surface and incubated for 30 min at room temperature. The spots were then washed with PBS for three times. The surface density of RGD-TGTs were checked by the quantification of Cy5 fluorophore before seeding of cells. Images were captured using a fluorescence microscope (Nikon) with a 20X air lens and a cooled CDD camera (Hamamatsu), and intensity of Cy5 fluorophore was measured using ImageJ software.

### 2.4. Immunofluorescent (IF) staining

Cells were fixed with 4% of paraformaldehyde in PBS, pH 7.4, for 30 min, followed by permeabilization with Tris-buffered saline containing 0.3% of Triton X-100 for 5 min. After blocking with 5.5% of normal goat serum for 30 min, samples were incubated overnight at 4 °C with antibodies, then for 1 h with secondary antibodies, phalloidin, and Hoechst, washed, mounted and examined on a fluorescence microscope (Nikon) with a 60X oil-immersion lens. Images were captured using a cooled CDD camera operated by (Hamamatsu) image acquisition software and arranged using Photoshop (Adobe) software.

### 2.5. Image analysis

For the quantification of FA length, the images of IF staining with anti-paxillin antibody were segmented and analyzed using ImageJ software. Briefly, a threshold, based on the background of fluorescence images, was used for the identification of FAs. Length of FAs in cells were determined by drawing the major axis of each individual FAs and measuring their lengths using the built-in function of ImageJ. The average of FA length per cell was calculated. The distribution of all FAs in each group was presented by box and whisker plots. The average of FA size of individual cells in each group was presented by scatter dot plots. For the analysis of the YAP nuclear translocation, the regions of whole cell and cell nucleus were drawn according to the DIC image and Hoechst staining, respectively. The fluorescence intensities of YAP signal in whole cell and nuclear region were also measured using ImageJ. The nuclear enrichment of YAP was presented as the ratio of background-subtracted fluorescence mean intensity for YAP in nuclear region to the one in the whole cell region.

## 3. Results

### 3.1. Molecular tension driven FA maturation in different size

To create the integrin ligand linked TGT, we conjugated the integrin

ligand cyclic-RGDfK peptide [39] to five different Cy5-labeled DNA TGTs (Fig. S1). These DNA tethers share the same length, sequence, and thermal stability, but have different $T_{tol}$ values, which were estimated to be 33, 43, 50, 54, and 56 pN [37]. The five RGD-conjugated TGTs were then immobilized through a neutravidin-biotin linker to the glass surface coated with biotin-BSA. The Because the avidin-biotin unbinding force is about 160 pN [40], the $T_{tol}$ values of these RGD-conjugated TGTs depend on the force application geometries of the TGT constructs. We

then plated MEFs on the surface of these RGD-conjugated TGTs, and examined the cell adhesion by phase-contrast images. Consistent with the results reported earlier [37], we observed that the threshold of molecular tension for initial cell adhesion was in the range of 33–43 pN. Cells were well attached on the TGTs with $T_{tol} \geq 43$ pN, but only very few cells were attached to 33 pN TGT. For TGT with $T_{tol}$ of 43 pN, cells spread slightly during the first 30 min; but did not continue to spread out thereafter. For TGTs with $T_{tol} \geq 50$ pN, cells attached within 15 min and
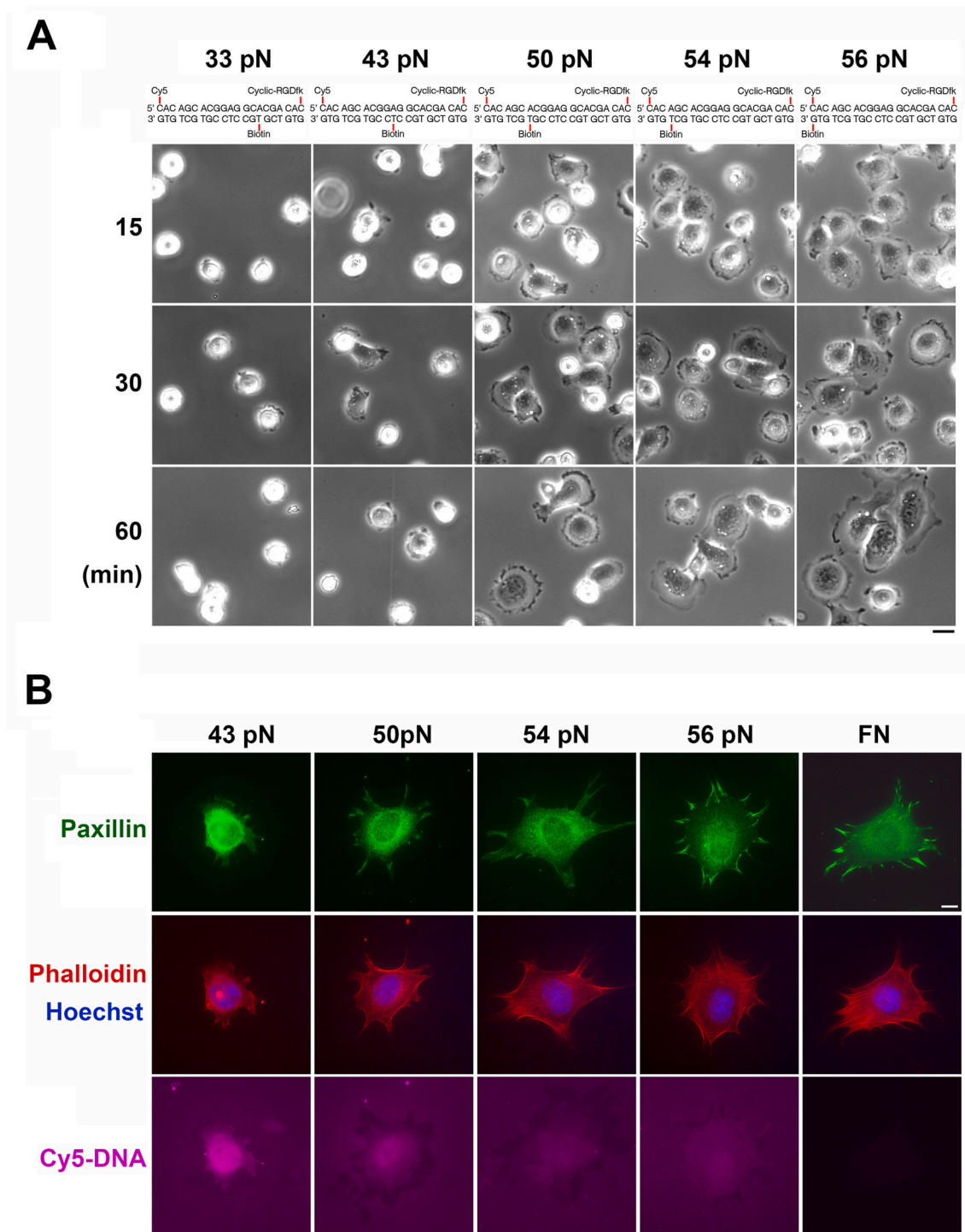


**Fig. 1.** The images of MEFs seeded on RGD-conjugated TGTs (A) The phase images of MEFs seeded on TGTs with $T_{tol}$ of 33–56 pN for 15–60 min. Scale bar, 20 μm. (B) Cells seeded on FN-coated coverslips or TGTs with $T_{tol}$ of 43–56 pN for 60 min were fixed and stained with anti-paxillin antibody (green) and phalloidin (red). The dsDNA-duplex was visualized by Cy5 (purple). Scale bar, 10 μm. (For interpretation of the references to colour in this figure legend, the reader is referred to the Web version of this article.)

continue to spread out thereafter (Fig. 1A). These data indicate that the molecular tension on integrins is about 43 pN for initial cell adhesion; the tension then increases gradually throughout the FA maturation during cell spreading.

To observe the formation of FAs and actin filaments, cells were fixed for IF staining with anti-paxillin antibody and phalloidin, respectively. MEFs seeded on the FN-coated glass coverslips was used here as a positive control. We found that MEFs formed FAs and well-organized actin filaments in the cells seeded on the TGTs with $T_{tol} \geq 50$ pN. The formation of FAs was enhanced slightly with increasing $T_{tol}$ of TGTs (Fig. 1B). As reported in several literatures [37,41,42], we observed the loss of Cy5 signal in some regions around the cells, indicating that TGT rupture occurs when integrin forces was larger than $T_{tol}$. It has been reported that treatment of cells with ROCK inhibitor Y27632 or myosin II inhibitor blebbistatin significantly abolished the rupture of TGTs with $T_{tol} \geq 43$ pN, but had no effect on TGTs with $T_{tol} \leq 33$ pN [42]. It suggests that forces across integrins and TGTs with $T_{tol} \geq 43$ pN are mediated by actomyosin contractility.

To measure the molecular forces required for FA maturation in different sizes, cells were fixed for IF staining with anti-paxillin antibody (Fig. 2A). The lengths of FAs were measured by ImageJ. We found only small focal adhesion complexes ($< 1$ μm) in cells seeded on 43 pN TGT for 30 min; FAs were not formed, and some cells became detached thereafter. For TGTs with $T_{tol} \geq 50$ pN, small FAs appeared in about 15 min, and the sizes of FAs increased with the increment of $T_{tol}$. Thereafter, the difference in FA sizes associated with different $T_{tol}$ was more pronounced. During the 60 min observation period, the sizes of FAs increase, up to the size of 2 μm, 3 μm, and 6 μm for $T_{tol}$ values of 50 pN, 54 pN, and 56 pN, respectively (Fig. 2B). We also calculated the average FA size in each individual cells, which shows a positive correlation between FA maturation and molecular tension on integrins (Fig. 2C). The data suggest that the molecular tension on integrins is enhanced gradually with the increase of FA size during the process of FA maturation. We also measured the cell area of MEFs seeded on these TGTs and found that the cell area was also sensitive to $T_{tol}$ of the TGTs (Fig. 2D). Cells were poor spreading on 43 pN TGT and well spreading on the TGTs with
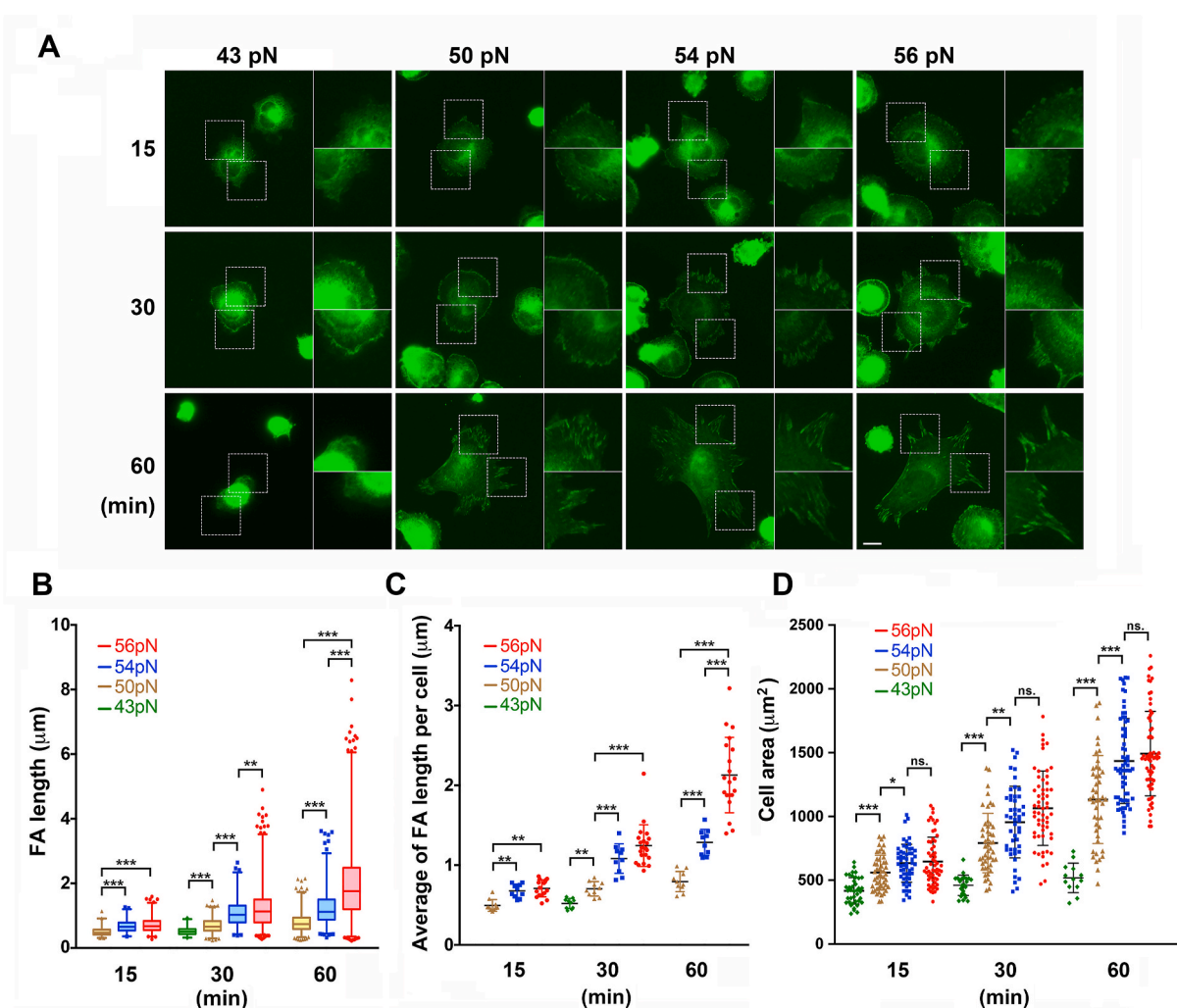


**Fig. 2.** Molecular forces required for FA maturation in different sizes. MEFs were seeded on RGD-conjugated TGTs with $T_{tol}$ of 43–56 pN for different durations as indicated. (A) Cells were fixed and stained with anti-paxillin antibody (green). One set of the represented images was shown. Scale bar, 10 μm. (B) Box and whisker diagrams showing the length of all detected FAs on TGTs with $T_{tol}$ of 43 pN (green), 50 pN (yellow), 54 pN (blue), and 56 pN (red) for 15–60 min as indicated ($> 500$ FAs from more than12 representative cells in three independent experiments). Boxplots represent 25th, 50th, and 75th percentiles, while whiskers extend to the 1st and 99th percentiles, outliers are plotted as individual dots. (C) Scatter dot plots show the average length of FA of each individual cells. Data are expressed as mean $\pm$ SD from more than 12 cells; each dot represents one single cell. (D) The cell area in different conditions was measured and presented by the scatter dot plots. Data are expressed as mean $\pm$ SD from more than 45 cells three independent experiments, except the 43 pN TGT groups. Differences between continuous variables were compared using the Mann-Whitney $U$ test. *P $< 0.05$; **P $< 0.005$; ***P $< 0.001$; ns., not statistically significant. (For interpretation of the references to colour in this figure legend, the reader is referred to the Web version of this article.)

$T_{tol} \geq 50$ pN. Cell area was significant increased with the increment of $T_{tol}$ in the range from 43 pN to 54 pN, while no statistical difference between cells on 54 pN and 56 pN TGTs regardless of incubation time. The similar ligand density on the surface of these TGTs were checked by measuring the Cy5 fluorescence intensity before seeding cells (Fig. S2), suggesting the observed cellular difference was not due to the ligand density RGD-TGTs but due to the $T_{tol}$ of the TGTs. In addition, the FA length and cell area of MEFs seeded on the surface of FN-coated glass were also measured (Fig. S3). Taken together, our data suggest that both FA size and cell spreading area are mechanosensitive in MEFs.
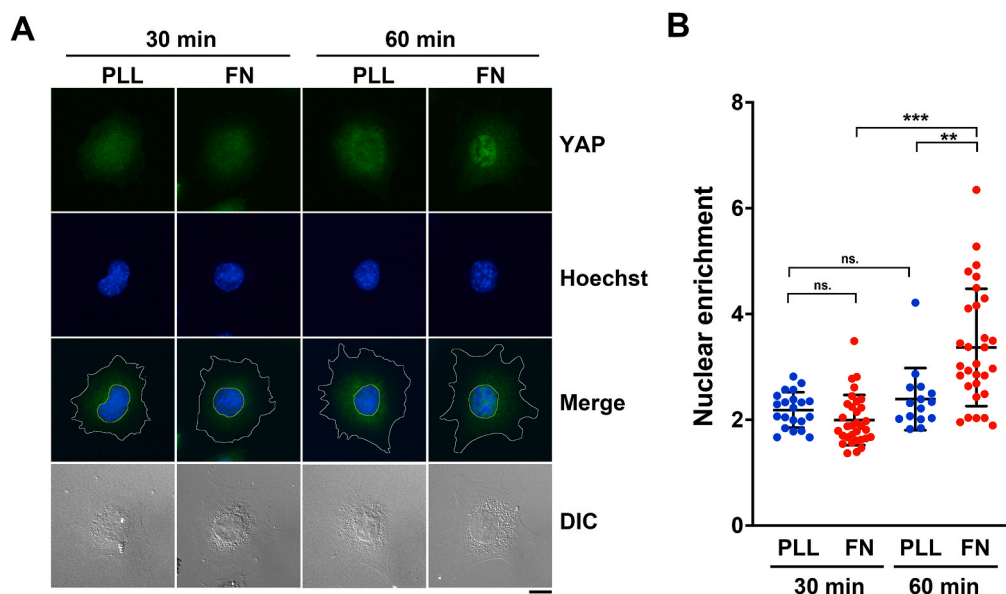
### 3.2. Molecular tension on integrin for YAP nuclear translocation

It is well known that the nuclear translocation of the transcriptional regulator YAP can be regulated by mechanical signaling [17,29]. Here, we used the RGD-conjugated TGTs to test if there is a threshold of molecular force required for YAP nuclear translocation. To examine whether it is dependent on integrins and to figure out the appropriate time of cell attachment for YAP nuclear translocation, MEFs were plated on the glass surface coated with PLL or FN for 30 and 60 min, followed by IF staining with anti-YAP antibody and Hoechst. Unlike FN which promotes cell attachment by activating integrins, PLL provides cell attachment without activation of integrins. We found that the distribution of YAP in cells was predominantly concentrated in the nuclei after cells were attached to FN for 60 min, while YAP was still evenly distributed in both nucleus and perinuclear cytoplasm in cells seeded on PLL, suggesting the dependence of integrin activation for YAP nuclear translocation. The nuclear enrichment of YAP was not observed in either FN- or PLL-attached cells at the 30-min time point, suggesting this event requiresmore than 30 min of cell attchment (Fig. 3).

We then plated MEFs on the surface of RGD-conjugated TGTs with $T_{tol}$ of 43–56 pN for 60 min to examine the molecular force on integrins required for YAP nuclear translocation. After 60 min of cell attachment, a significant nuclear enrichment of YAP was observed in the cells seeded on TGTs with $T_{tol} \geq 54$ pN, but not in the cells seeded on TGTs with $T_{tol} \leq 50$ pN (Fig. 4), suggesting that the threshold of molecular tension across integrins required for YAP nuclear translocation was in the range of 50–54 pN during cell attachment.

## 4. Discussion

Mechanical forces are essential for a variety of cellular processes through the activation of a wide variety of mechanosensitive signal pathways. In this study, we used the RGD-conjugated TGT approach to determine the requirement of molecular tension on integrins for FA maturation in different sizes. The integrins bond to the tethered ligand, and FAs are formed and matured only if the tether does not rupture. Our results show that the limitation of FA sizes in cells seeded on TGTs with different $T_{tol}$ were less than 1 μm, 2 μm, 3 μm, and 6 μm for $T_{tol}$ values of 43 pN, 50 pN, 54 pN, and 56 pN, respectively. It is well known that YAP nuclear translocation requires the activation of integrins and the myosin II-mediated contractility. However, it is not clear if there is a threshold of molecular tension for this mechanosensitive event. Here, we observed that YAP was significantly enriched in the nuclei of cells adhere on the surface of 54 pN TGT, but not on 50 pN TGT. Our data suggest that the threshold of molecular force requirement on integrins for YAP nuclear translocation take place was in the range of 50–54 pN.

Many literatures report that nascent adhesion formation is myosin II-independent, whereas FA maturation is myosin II-dependent [11,16, 43]. It has been reported that the molecular tension threshold fall within the range from 33 pN to 43 pN for integrin activation during initial adhesion. This tension threshold was reduced when cells were treated with hypertonic medium, but was not affected by the treatment of myosin II inhibitor blebbistatin in CHO–K1 cells [37], suggesting the molecular tension for initial stages of cell adhesion is regulated by membrane tension but not by actomyosin contractility. In our study, we observed the same range of molecular tension for initial cell adhesion in MEFs. However, only small FAs appeared in the MEFs seeded on 43 pN TGT. It suggests that molecular tension required for nascent adhesion formation is less than 43 pN, but that larger tension is required for FA maturation in MEFs. Reminiscent of two previous studies, the assembly of nascent adhesions at the leading edge of migrating cells was found to be independent of substrate rigidity or cell contractility [44]; and nascent adhesions are responsible for the generation of propulsive forces in migrating fibroblasts [45]. We speculate that the tension thresholds for initial adhesion and for FA formation may be mainly regulated by different cellular determinants, the former being the cell membrane and the latter the cytoskeleton. All of these might be influenced by the cellular context and the spatiotemporal dynamics under different conditions.

It is well known that the formation of matured FAs involves multiple proteins and requires mechanical stimulus [46,47]. By plating MEFs on FN-coated polyacrylamide gels with different rigidity, we have demonstrated that FA maturation in MEFs depends on the matrix stiffness and



**Fig. 3.** Integrin activation is critical for YAP nuclear localization. MEFs were plated on PLL- or FN-coated coverslips for 30 min or 60 min. (A) Cells were fixed and stained with anti-YAP antibody (green). Nuclei were stained with Hoechst (blue). Cell morphology is displayed by DIC images. The cell boundary is shown in white and the nuclei boundary in yellow. Scale bar, 10 μm. (B) Scatter dot plots of nuclear enrichment of YAP. Data are expressed as mean ± SD from more than 15 representative cells on PLL and 30 representative cells on FN in three independent experiments; each dot represents one single cell. Differences between continuous variables were compared using the Mann-Whitney $U$ test. **P < 0.005; ***P < 0.0005; ns., not statistically significant. (For interpretation of the references to colour in this figure legend, the reader is referred to the Web version of this article.)
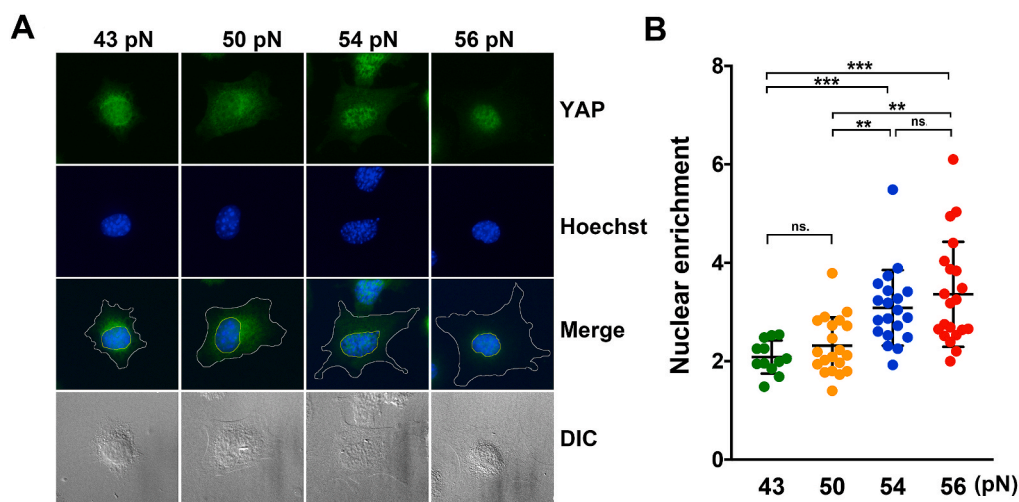
**Fig. 4.** The molecular forces required for YAP nuclear localization. (A) MEFs seeded on RGD-conjugated TGTs with $T_{tol}$ of 43–56 pN for 60 min were fixed and IF stained with anti-YAP antibody (green). Cell nuclei were stained with Hoechst (blue). Cell morphology is displayed by DIC images. The cell boundary is shown in white and the nuclei boundary in yellow. Scale bar, 10 μm. (B) Scatter dot plots of YAP nuclear enrichment. Data are expressed as mean ± SD from 12 cells on 43 pN TGT and 20 cells on 50–56 pN TGTs in three independent experiments; each dot represents one single cell. Differences between continuous variables were compared using the Mann-Whitney $U$ test. **P < 0.005; ***P < 0.0005; ns., not statistically significant. (For interpretation of the references to colour in this figure legend, the reader is referred to the Web version of this article.)

correlates with the enhanced stress fibers and intracellular traction forces [48]. In this study, we found that the requirement of molecular force increased gradually as FA size increased. MEFs on TGTs with $T_{tol} \geq$ 50 pN started to form FAs within 15 min and expanded over time to varying degrees depending on $T_{tol}$ of TGTs, whereas MEFs on 43 pN TGT only formed small FAs at the 30-min time points. We also found that the cell spreading area of MEFs seeded on TGTs was sensitive to $T_{tol}$ of the TGTs. One recent study has reported that cell spreading area was sensitive to substrate stiffness in NIH 3T3 fibroblasts [49]. They demonstrated that cells seeded on soft substrates exhibited normal protrusion activity, but these protrusions were not stabilized due to impaired adhesion assembly, resulting in poor spreading. Here, we found that MEFs were poor spreading on 43 pN TGT, that might be very similar to the condition of cells seeded on soft substrates.

The loss of Cy5 signal of DNA tethers represents the rupture of DNA duplex tethers caused by exceeding forces as reported in several literatures [37,41,42]. In our study, we also observed this feature which allows us to confirm that the observed events, such as the detected FA and YAP nuclear translocation must have occurred at the tension below the $T_{tol}$ of the corresponding TGTs. However, the drawback is that cells could detach from the TGTs with low $T_{tol}$. The multiplex TGT (mTGT) approach [41] and the quenched tension gauge tether (qTGT) approach [50] can simultaneously monitor multiple levels of integrin-mediated molecular tension over a wide time scale during the onset of adhesion and cell migration. Another DNA-based digital tension probes have been developed using DNA hairpins with predictable secondary structure and fluorophore-quencher pair in the designated positions [51]. The probes serve as a switch to generate a significant increase in fluorescence intensity when the tension is higher than the threshold for hairpin un-winding. This design strategy provides a way to monitor the real-time molecular tension during cell spreading. The combination of RGD-ligand-DNA tension sensors with super-resolution imaging technology takes the study of cell mechanics to another ultrastructure level [52–55]. In our study, we observed that the requirement of molecular tension on integrins is positively correlated with FA size. It implies that the tension magnitudes in the FA structure may not be evenly distributed throughout the FA maturation. Integrating these methods and research results will help us to further understand the underlying network of mechanotransduction.

## 5. Conclusions

Using the RGD-DNA TGT approach, we demonstrated that the molecular tension on integrins required for FA maturation in different sizes increased as FA size increased. Specifically, we showed that the limitation of FA sizes in cells seeded on TGTs with different $T_{tol}$ were less than 1 μm, 2 μm, 3 μm, and 6 μm for $T_{tol}$ values of 43 pN, 50 pN, 54 pN, and 56 pN, respectively. For YAP nuclear translocation, we quantified that the threshold of molecular tension on integrin for this event to take place was in the range of 50–54 pN.

## Declaration of interests

The authors declare that they have no known competing financial interests or personal relationships that could have appeared to influence the work reported in this paper.

## Appendix A. Supplementary data

Supplementary data to this article can be found online at https://doi.org/10.1016/j.bbrep.2022.101287.

## References

[1] D.E. Ingber, Integrins, tensegrity, and mechanotransduction, Gravit Space Biol Bull 10 (2) (1997) 49–55.

[2] N. Wang, J.D. Tytell, D.E. Ingber, Mechanotransduction at a distance: mechanically coupling the extracellular matrix with the nucleus, Nat. Rev. Mol. Cell Biol. 10 (1) (2009) 75–82.

[3] D.E. Jaalouk, J. Lammerding, Mechanotransduction gone awry, Nat. Rev. Mol. Cell Biol. 10 (1) (2009) 63–73.

[4] D.E. Discher, P. Janmey, Y.L. Wang, Tissue cells feel and respond to the stiffness of their substrate, Science 310 (5751) (2005) 1139–1143.

[5] M.A. Wozniak, C.S. Chen, Mechanotransduction in development: a growing role for contractility, Nat. Rev. Mol. Cell Biol. 10 (1) (2009) 34–43.

[6] K.S. Kolahi, M.R. Mofrad, Mechanotransduction: a major regulator of homeostasis and development, Wiley Interdiscip Rev Syst Biol Med 2 (6) (2010) 625–639.

[7] M.A. Schwartz, D.W. DeSimone, Cell adhesion receptors in mechanotransduction, Curr. Opin. Cell Biol. 20 (5) (2008) 551–556.

[8] B. Geiger, J.P. Spatz, A.D. Bershadsky, Environmental sensing through focal adhesions, Nat. Rev. Mol. Cell Biol. 10 (1) (2009) 21–33.

[9] M.L. Gardel, et al., Mechanical integration of actin and adhesion dynamics in cell migration, Annu. Rev. Cell Dev. Biol. 26 (2010) 315–333.

[10] A. del Rio, et al., Stretching single talin rod molecules activates vinculin binding, Science 323 (5914) (2009) 638–641.

[11] Parsons, J.T., A.R. Horwitz, and M.A. Schwartz, Cell adhesion: integrating cytoskeletal dynamics and cellular tension. Nat. Rev. Mol. Cell Biol.. 11(9): p. 633-643.

[12] D.J. Webb, J.T. Parsons, A.F. Horwitz, Adhesion assembly, disassembly and turnover in migrating cells – over and over and over again, Nat. Cell Biol. 4 (4) (2002) E97–E100.

[13] S. Huveneers, E.H. Danen, Adhesion signaling - crosstalk between integrins, Src and Rho, J. Cell Sci. 122 (Pt 8) (2009) 1059–1069.

[14] R. Zaidel-Bar, et al., Functional atlas of the integrin adhesome, Nat. Cell Biol. 9 (8) (2007) 858–867.

[15] A. Elosegui-Artola, X. Trepat, P. Roca-Cusachs, Control of mechanotransduction by molecular clutch dynamics, Trends Cell Biol. 28 (5) (2018) 356–367.

[16] F. Martino, et al., Cellular mechanotransduction: from tension to function, Front. Physiol. 9 (2018) 824.

[17] G. Halder, S. Dupont, S. Piccolo, Transduction of mechanical and cytoskeletal cues by YAP and TAZ, Nat. Rev. Mol. Cell Biol. 13 (9) (2012) 591–600.

[18] P. Strzyz, Mechanotransduction: enforcing protein import, Nat. Rev. Mol. Cell Biol. 18 (12) (2017) 713.

[19] T. Moroishi, C.G. Hansen, K.L. Guan, The emerging roles of YAP and TAZ in cancer, Nat. Rev. Cancer 15 (2) (2015) 73–79.

[20] S.W. Plouffe, A.W. Hong, K.L. Guan, Disease implications of the Hippo/YAP pathway, Trends Mol. Med. 21 (4) (2015) 212–222.

[21] S. Porazinski, et al., YAP is essential for tissue tension to ensure vertebrate 3D body shape, Nature 521 (7551) (2015) 217–221.

[22] B. Zhao, et al., The Hippo-YAP pathway in organ size control and tumorigenesis: an updated version, Genes Dev. 24 (9) (2010) 862–874.

[23] T. Panciera, et al., Mechanobiology of YAP and TAZ in physiology and disease, Nat. Rev. Mol. Cell Biol. 18 (12) (2017) 758–770.

[24] Z. Meng, T. Moroishi, K.L. Guan, Mechanisms of Hippo pathway regulation, Genes Dev. 30 (1) (2016) 1–17.

[25] M. Aragona, et al., A mechanical checkpoint controls multicellular growth through YAP/TAZ regulation by actin-processing factors, Cell 154 (5) (2013) 1047–1059.

[26] F. Calvo, et al., Mechanotransduction and YAP-dependent matrix remodelling is required for the generation and maintenance of cancer-associated fibroblasts, Nat. Cell Biol. 15 (6) (2013) 637–646.

[27] S. Dupont, et al., Role of YAP/TAZ in mechanotransduction, Nature 474 (7350) (2011) 179–183.

[28] A. Elosegui-Artola, et al., Mechanical regulation of a molecular clutch defines force transmission and transduction in response to matrix rigidity, Nat. Cell Biol. 18 (5) (2016) 540–548.

[29] A. Elosegui-Artola, et al., Force triggers YAP nuclear entry by regulating transport across nuclear pores, Cell 171 (6) (2017) 1397–1410, e14.

[30] C.M. Kraning-Rush, et al., Quantifying traction stresses in adherent cells, Methods Cell Biol. 110 (2012) 139–178.

[31] R.W. Style, et al., Traction force microscopy in physics and biology, Soft Matter 10 (23) (2014) 4047–4055.

[32] Y. Liu, et al., Molecular tension probes for imaging forces at the cell surface, Acc. Chem. Res. 50 (12) (2017) 2915–2924.

[33] M. Morimatsu, et al., Molecular tension sensors report forces generated by single integrin molecules in living cells, Nano Lett. 13 (9) (2013) 3985–3989.

[34] L.S. Fischer, et al., Molecular force measurement with tension sensors, Annu. Rev. Biophys. 50 (2021) 595–616.

[35] C. Grashoff, et al., Measuring mechanical tension across vinculin reveals regulation of focal adhesion dynamics, Nature 466 (7303) (2010) 263–266.

[36] T.R. Ham, K.L. Collins, B.D. Hoffman, Molecular tension sensors: moving beyond force, Curr Opin Biomed Eng 12 (2019) 83–94.

[37] X. Wang, T. Ha, Defining single molecular forces required to activate integrin and notch signaling, Science 340 (6135) (2013) 991–994.

[38] F. Chowdhury, et al., Single molecular force across single integrins dictates cell spreading, Integr Biol (Camb) 7 (10) (2015) 1265–1271.

[39] E. Ruoslahti, RGD and other recognition sequences for integrins, Annu. Rev. Cell Dev. Biol. 12 (1996) 697–715.

[40] V.T. Moy, E.L. Florin, H.E. Gaub, Intermolecular forces and energies between ligands and receptors, Science 266 (5183) (1994) 257–259.

[41] Y. Wang, X. Wang, Integrins outside focal adhesions transmit tensions during stable cell adhesion, Sci. Rep. 6 (2016), 36959.

[42] X. Wang, et al., Integrin molecular tension within motile focal adhesions, Biophys. J. 109 (11) (2015) 2259–2267.

[43] A.M. Pasapera, et al., Myosin II activity regulates vinculin recruitment to focal adhesions through FAK-mediated paxillin phosphorylation, J. Cell Biol. 188 (6) (2010) 877–890.

[44] R. Changede, et al., Nascent integrin adhesions form on all matrix rigidities after integrin activation, Dev. Cell 35 (5) (2015) 614–621.

[45] K.A. Beningo, et al., Nascent focal adhesions are responsible for the generation of strong propulsive forces in migrating fibroblasts, J. Cell Biol. 153 (4) (2001) 881–888.

[46] J.C. Kuo, et al., Analysis of the myosin-II-responsive focal adhesion proteome reveals a role for beta-Pix in negative regulation of focal adhesion maturation, Nat. Cell Biol. 13 (4) (2011) 383–393.

[47] L.B. Case, et al., Molecular mechanism of vinculin activation and nanoscale spatial organization in focal adhesions, Nat. Cell Biol. 17 (7) (2015) 880–892.

[48] H.H. Lee, et al., Shp2 plays a crucial role in cell structural orientation and force polarity in response to matrix rigidity, Proc. Natl. Acad. Sci. U. S. A. 110 (8) (2013) 2840–2845.

[49] P.W. Oakes, et al., Lamellipodium is a myosin-independent mechanosensor, Proc. Natl. Acad. Sci. U. S. A. 115 (11) (2018) 2646–2651.

[50] M.H. Jo, W.T. Cottle, T. Ha, Real-time measurement of molecular tension during cell adhesion and migration using multiplexed differential analysis of tension gauge tethers, ACS Biomater. Sci. Eng. 5 (8) (2019) 3856–3863.

[51] Y. Zhang, et al., DNA-based digital tension probes reveal integrin forces during early cell adhesion, Nat. Commun. 5 (2014) 5167.

[52] T. Schlichthaerle, C. Lindner, R. Jungmann, Super-resolved visualization of single DNA-based tension sensors in cell adhesion, Nat. Commun. 12 (1) (2021) 2510.

[53] J.M. Brockman, et al., Live-cell super-resolved PAINT imaging of piconewton cellular traction forces, Nat. Methods 17 (10) (2020) 1018–1024.

[54] Y. Zhao, et al., Cellular force nanoscopy with 50 nm resolution based on integrin molecular tension imaging and localization, J. Am. Chem. Soc. 142 (15) (2020) 6930–6934.

[55] A. Blanchard, et al., Turn-key mapping of cell receptor force orientation and magnitude using a commercial structured illumination microscope, Nat. Commun. 12 (1) (2021) 4693.